

**Two-photon pulse-scattering spectroscopy for arrays of two-level atoms coupled to a waveguide**Ekaterina Vlasiuk<sup>1</sup>, Alexander V. Poshakinskiy<sup>2</sup>, and Alexander N. Poddubny<sup>3,\*</sup><sup>1</sup>*Department of Physics, University of Basel, Klingelbergstrasse 82, CH-4056 Basel, Switzerland*<sup>2</sup>*Ioffe Institute, St. Petersburg 194021, Russia*<sup>3</sup>*Department of Physics of Complex Systems, Weizmann Institute of Science, Rehovot 7610001, Israel*

(Received 26 March 2023; revised 8 August 2023; accepted 24 August 2023; published 8 September 2023)

We theoretically studied the scattering of short two-photon pulses from a spatially separated array of two-level atoms coupled to the waveguide. A general analytical expression for the scattered pulse has been obtained. The contributions of various single-eigenstate and double-excited eigenstates of the array have been analyzed. We also calculated how the time, during which the incident photons are stored in the array, depends on the array period and the number of atoms. The largest storage times correspond to the structures with the anti-Bragg period, equal to the quarter of the wavelength of light at the atom resonance frequency  $\lambda/4$ .

DOI: [10.1103/PhysRevA.108.033705](https://doi.org/10.1103/PhysRevA.108.033705)**I. INTRODUCTION**

Waveguide quantum electrodynamics (WQED), focused on light-matter interactions in arrays of natural or artificial atoms that are coupled to the waveguide, is a rapidly developing field of quantum optics [1,2]. Multiple experimental platforms to study fundamental physics models and engineer atom-photon interactions have now emerged. Among the recent experimental results in the field of WQED are the demonstrations of photon bound states [3] and photon squeezing [4] in the low-excitation regime, as well as observation of the superradiant burst for the strongly excited arrays [5,6]. Practical applications such as detection, processing [3], and generation [7] of quantum photon states would ultimately require devices operating in the pulsed regime. Hence, there is a fundamental need for a deeper understanding the time-dependent atom-photon interaction in this system.

In fact, a general scattering matrix consideration of the photon scattering on an array of atoms in one point has already been performed in the first works in the field [8,9]. Additionally, the time dependence of the scattered two-photon wave function and the manifestation of the photon bound state in a single-atom case was analyzed in Ref. [10]. More recent studies have also investigated the formation of bound photon states in the time-dependent photon transmission for the two-atom case [11] as well as the many-atom case [12–15]. It has been predicted that the outgoing wave function can manifest not only bound photon states, but also more complex correlated multiphoton states formed due to atom-photon interactions [16]. One other important aspect of the photon-atom interactions is the quantum entanglement. In particular, time-energy entanglement in the scattered two-photon wave function for a cavity with an atom coupled to a waveguide has been theoretically considered in Ref. [17]. The scattering of a

time-entangled photon pulse was considered in Refs. [18,19]. Much attention is now attracted to the nonclassical photon emission from strongly driven atomic arrays [20,21].

However, there is one interesting aspect of the time-dependent photon transmission through the arrays, that has so far not been analyzed in detail to the best of our knowledge. That is the role of different collective states of the array. In particular, it is now well known that spatially separated arrays have a complicated structure of collective single- and double-excited states [22–25]. These states can be distinguished by their spontaneous decay rate, which can be either enhanced (for superradiant states) or suppressed (for subradiant states) due to the interference between the photons emitted from different atoms. It is then natural to examine the signatures of these states in the photon time dynamics. We recently analyzed the case of continuous wave excitation in detail in Refs. [26,27]. Here we focus on the case of excitation with a short pulse propagating through the array, see Fig. 1. We show that the measurement of the time-dependent joint detection probability of transmitted photons provides additional information about the double-excited collective modes that is harder to capture by the continuous excitation scheme. Specifically, the short pulse can excite both super and subradiant states, and the latter are naturally observed as long-living tails in the scattering dynamics. Frequency-domain observation of subradiant states is also possible but requires careful resonant tuning of incident light frequency. While this has been demonstrated for single-excited states [28], we are not yet aware of such results for the double-excited states excepting Ref. [29] for a rather special setup of two coupled qubit pairs. Thus, we hope that this work could be useful both as a first step for potential future analysis of a multiphoton pulsed regime and as a helpful tool for the analysis of ongoing and future experiments [30,31]. For example, the longer-living tails of the superradiant burst reported in Ref. [6] could be interpreted as signatures of subradiant states.

The rest of the paper is organized as follows. Section II outlines our model and the calculation approach. Next, we

\*poddubny@weizmann.ac.il

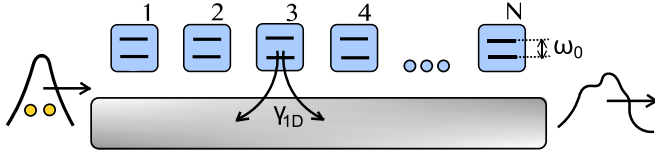


FIG. 1. Schematics of a two-photon pulse propagating through an array of qubits coupled to a waveguide. Here,  $\omega_0$  is a resonant frequency of qubits and  $\gamma_{1D}$  is a spontaneous emission rate into the guided mode.

present the results for the two-photon wave function in Sec. III. Our main results are summarized in Sec. IV. Appendix A is reserved for auxiliary theoretical details.

## II. MODEL AND CALCULATION APPROACH

We consider a basic WQED setup with  $N$  two-level qubits, periodically spaced near a waveguide and interacting via a waveguide mode. The system is schematically shown in Fig. 1 and can be described by the following effective Hamiltonian [1,23,32]:

$$H = -i\gamma_{1D} \sum_{n,m=1}^N \sigma_n^\dagger \sigma_m e^{i(\omega_0/c)|z_m - z_n|}. \quad (1)$$

This Hamiltonian assumes the usual Markovian and rotating-wave approximations. The raising operators  $\sigma_m^\dagger$  obey the usual spin-1/2 operators algebra:  $\sigma_m^2 = 0$ ,  $\sigma_m \sigma_m^\dagger + \sigma_m^\dagger \sigma_m = 1$ ,  $[\sigma_m, \sigma_n] = 0$  for  $m \neq n$ . The energy is counted from the atomic resonance  $\hbar\omega_0$ ,  $c$  is the speed of light, and  $z_m$  are the qubit coordinates along the waveguide. For a periodic array, where  $z_{m+1} - z_m = d$ , the period can be conveniently characterized just by a single dimensionless parameter, the phase  $\varphi = \omega_0 d/c \equiv 2\pi d/\lambda_0$  gained by the light between two neighboring two-level atoms with the distance  $d$ . An important feature of the Hamiltonian Eq. (1) is the long-ranged coupling between distant atoms, mediated by the waveguide photons. The model assumes that the propagating photon amplitude does not decay with distance and just acquires a phase  $(\omega_0/c)|z_m - z_n|$ , which governs the coupling between the atoms  $m$  and  $n$ . The parameter  $\gamma_{1D}$  is the radiative decay rate of a single atom into the waveguide. It is because of this spontaneous decay that the effective Hamiltonian is non-Hermitian.

We are interested in the scattering of a general two-photon state, characterized by a time-dependent wave function  $\psi_{t_1, t_2}^{\text{in}}$  from such a setup. To this end, we use the known general technique [23,33–35] to calculate the two-photon scattering matrix in the frequency domain  $S(\omega'_1, \omega'_2 \leftarrow \omega_1, \omega_2)$ . We start with the Fourier transform of the input state

$$\psi_{\omega_1, \omega_2}^{\text{in}} = \iint dt_1 dt_2 e^{i\omega_1 t_1} e^{i\omega_2 t_2} \psi_{t_1, t_2}^{\text{in}}. \quad (2)$$

The output state is then given by

$$\psi_{\omega'_1, \omega'_2}^{\text{out}} = \frac{1}{2} \iint \frac{d\omega_1 d\omega_2}{(2\pi)^2} S(\omega'_1, \omega'_2 \leftarrow \omega_1, \omega_2) \psi_{\omega_1, \omega_2}^{\text{in}} g, \quad (3)$$

and then we perform the inverse Fourier transform

$$\psi_{t_1, t_2}^{\text{out}} = \iint \frac{d\omega'_1 d\omega'_2}{(2\pi)^2} e^{-i\omega'_1 t_1} e^{-i\omega'_2 t_2} \psi_{\omega'_1, \omega'_2}^{\text{out}}. \quad (4)$$

The detailed derivation of the scattering matrix for an arbitrary number and positions of the qubits, mostly following Refs. [23,34], can be found, e.g., in Ref. [1]. Here we just recall the answer:

$$\begin{aligned} S(\omega'_1, \omega'_2 \leftarrow \omega_1, \omega_2) &= (2\pi)^2 t_{\omega_1, \omega_2} [\delta(\omega_1 - \omega'_1) \delta(\omega_2 - \omega'_2) \\ &+ \delta(\omega_1 - \omega'_2) \delta(\omega_2 - \omega'_1)] \\ &+ 2\gamma_{1D}^2 \sum_{m,n=1}^N s_m^-(\omega'_1) s_m^-(\omega'_2) [\Sigma^{-1}]_{mn} s_n^+(\omega_1) s_n^+(\omega_2) \\ &\times 2\pi \delta(\omega_1 + \omega_2 - \omega'_1 - \omega'_2), \end{aligned} \quad (5)$$

where

$$\Sigma_{mn}(\varepsilon) = \int G_{mn}(\omega) G_{mn}(2\varepsilon - \omega) \frac{d\omega}{2\pi} \quad (6)$$

is the self-energy matrix for double-excited states with  $G_{ij}$  being the Green's function for a single excitation of the array, given by the inverse of the following matrix:

$$\begin{aligned} [G^{-1}(\omega)]_{mn} &\equiv \omega \delta_{mn} - H_{mn} \\ &= (\omega - \omega_0) \delta_{mn} + i\gamma_{1D} e^{i(\omega_0/c)|z_m - z_n|}. \end{aligned} \quad (7)$$

The coefficients

$$s_m^\pm(\omega) = \sum_n G_{mn} e^{\pm i(\omega_0/c)z_n} \quad (8)$$

describe the coupling of the array with the incoming and outgoing plane waves. The first term in the scattering matrix (5) accounts for the independent photon transmission with the transmission coefficients given by

$$t_\omega = 1 - i\gamma_{1D} \sum_{mn} G_{mn} e^{i(\omega_0/c)(z_n - z_m)}. \quad (9)$$

The second term in Eq. (5) accounts for the interaction between the photons induced by the array.

For a general pulse shape, the integration over time and frequency can be performed only numerically and is rather tedious. However, it is greatly simplified for a short pulse when the input state  $\psi_{t_1, t_2}^{\text{in}}$  can be approximated by a product of two  $\delta$  functions

$$\psi_{t_1, t_2}^{\text{in}} = \delta(t_1) \delta(t_2). \quad (10)$$

Physically, this means that the pulse duration is significantly shorter than the inverse rate decay of the fastest eigenmode of the system, that is, on the order of  $1/(N\gamma_{1D})$ . From now on we restrict ourselves to such a case. The calculation procedure is detailed in Appendix A.

## III. TRANSMITTED PULSE

We start this section by analyzing in detail the wave function for the pulse, transmitted through the subwavelength array of a given length  $N = 4$ . Next, in Sec. III B, we examine

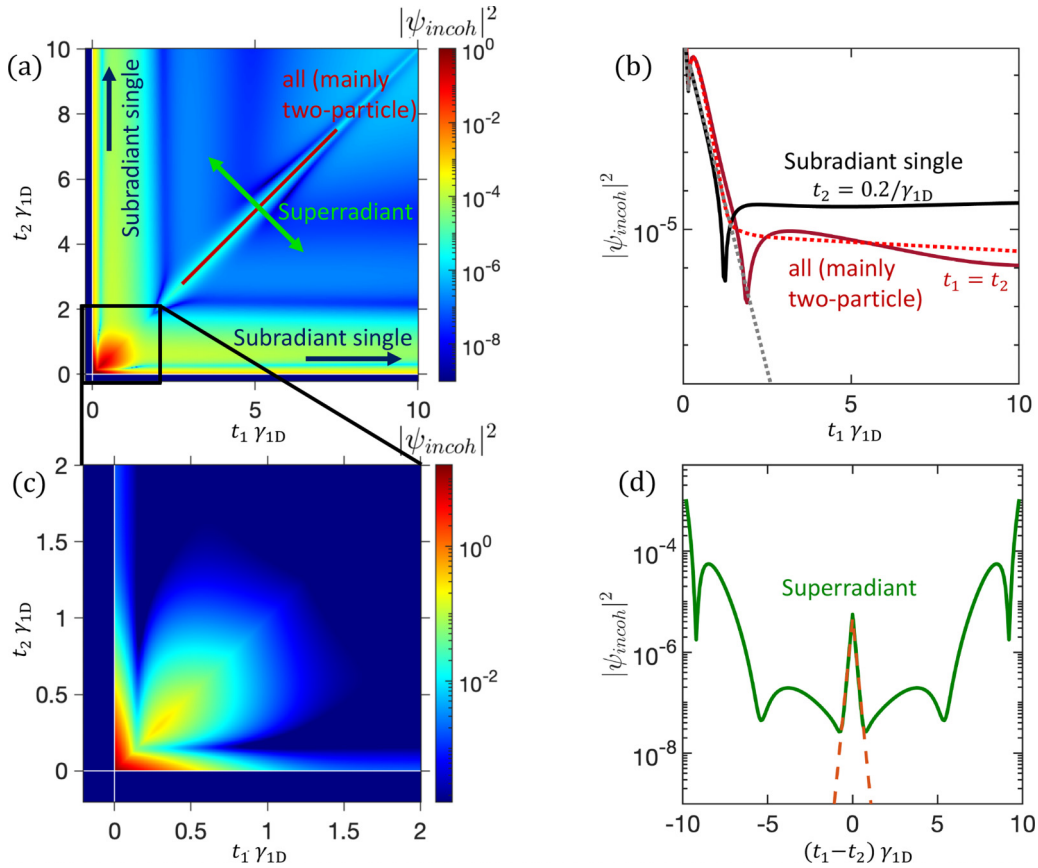


FIG. 2. Incoherent part of the transmitted pulse for the incident delta pulse in the time domain. Calculation is performed for  $N = 4$  and  $\varphi = 0.1$ . Times are normalized by  $1/\gamma_{1D}$ . (a) Schematics of the various types of photon states in the transmitted pulse. (b) Dark red solid curve: probability distribution to detect two photons at the same moment in time  $t_1$ . Black solid curve: probability distribution to detect one photon at the time  $t_1$  while the second photon is detected at time  $t_2 = 0.2/\gamma_{1D}$ . Dotted curves are calculated with all two-particle modes and only the superradiant single-particle mode; the red one is for the times  $t_1 = t_2$ , the gray one for the fixed  $t_2 = 0.2/\gamma_{1D}$ . (c) Zoomed-in image from panel (a). (d) Dependence of the probability of the two photons detection on the time difference  $t_1 - t_2$  for fixed  $t_1 + t_2 = 10/\gamma_{1D}$ . The solid green curve is calculated exactly, and the dashed orange curve includes only the superradiant single-excited state and all double-excited ones.

the dependence of the effective time it takes the system to scatter photons on the array length  $N$ .

### A. Single- and double-excited states in the transmitted pulse

Figure 2 shows the incoherent part of the two-photon wave function given by Eq. (A15) calculated under the incidence of the two-photon  $\delta$ -pulse Eq. (10). The incoherent part has quite a complicated time dependence with several distinct timescales. The shortest time scale  $t \sim 1/(N\gamma_{1D})$  corresponds to the superradiant state where the constructive interference enhances the emission rate. The longest timescale is on the order of  $N^3/(\varphi^2\gamma_{1D})$  [22] and corresponds to the excitation of subradiant states. To represent different timescales better, we show the wave function at large and short times in Figs. 2(a) and 2(c) separately.

For reference, we also present in Fig. 4 the complex spectrum of the system eigenfrequencies, calculated for the same system parameters as in Fig. 2. The orange dots correspond to the single-excited states. They were obtained as eigenvalues of the effective Hamiltonian matrix  $H_{mn}$ , defined in Eq. (7). The brightest state, with the largest imaginary part, corresponds to the superradiant state with the decay rate  $\approx N\gamma_{1D}$ . The three

other dots correspond to the single-excited subradiant states. The blue dots show the spectrum of double-excited states. This is calculated following Ref. [23]. The eigenfrequencies are found by diagonalizing Eq. (A4), given in the Appendix. The calculation demonstrates that there exists one superradiant mode, two subradiant ones, and also three modes with decay rates on the order of  $\gamma_{1D}$ . As discussed in Ref. [23], these three eigenstates could be understood as the “twilight” states, which are a product of the wave function with one photon being in the bright state and the other one being in the subradiant one.

Our calculation approach, outlined in detail in Appendix A, allows us to evaluate the contributions from various single- and double-excited eigenstates into the total transmitted wave function  $\psi(t_1, t_2)$  separately. Generally, the single-excited states manifest themselves in the dependence on  $t_1$  and  $t_2$ , that is, along the edges of the color map in Fig. 2(a). The double-excited states correspond to the dependencies on  $t_1 \pm t_2$ , that is, diagonal and antidiagonal in Fig. 2(a). Hence, the role of different contributions can be singled out by examining the cross sections in the corresponding directions, shown in Figs. 2(b) and 2(d). Our analysis of the contributions of various super and subradiant eigenstates and the directions, along

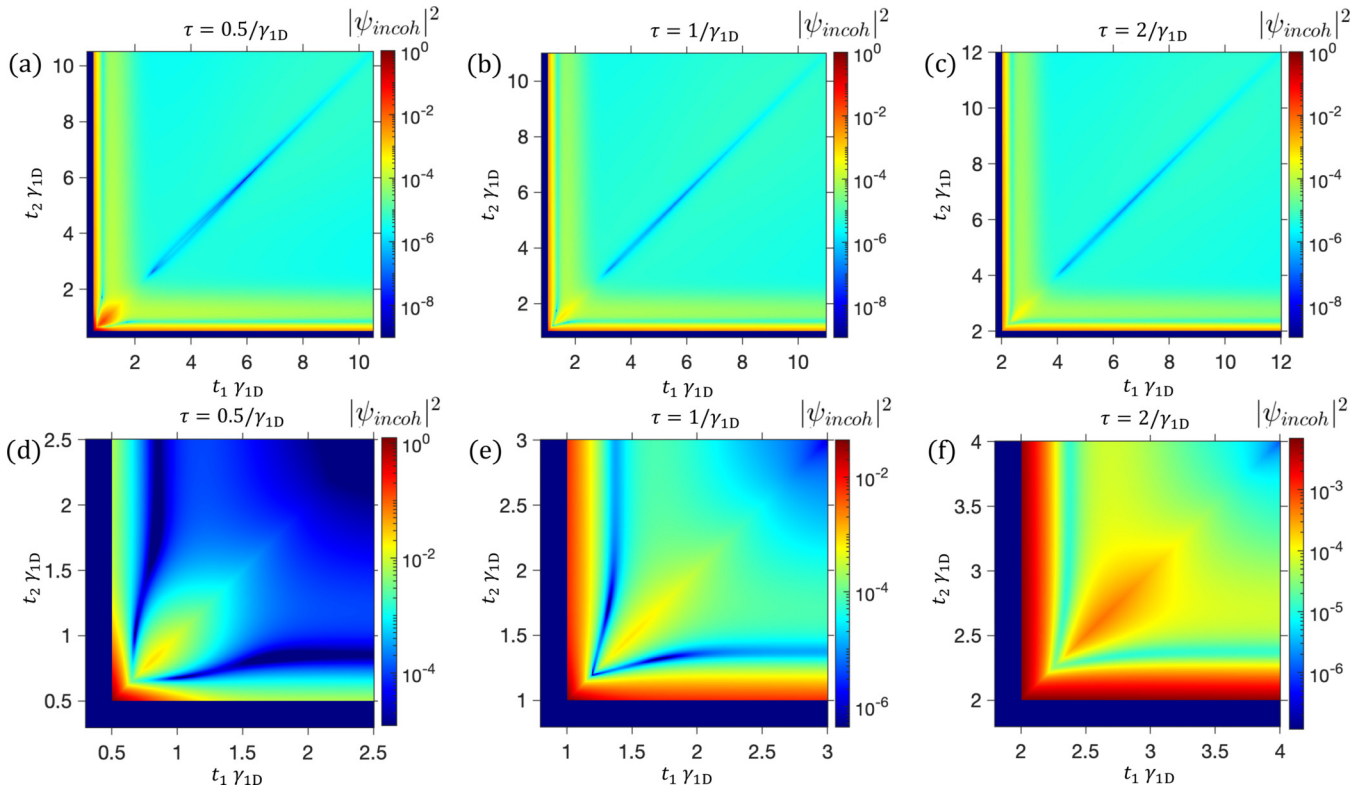


FIG. 3. Incoherent part of the transmitted pulse for the two short one-photon pulses incident with a time delay  $\tau$  [(a), (d):  $\tau = 0.5/\gamma_{1D}$ ; (b), (e):  $\tau = 1/\gamma_{1D}$ ; (c), (f):  $\tau = 2/\gamma_{1D}$ ] in the time domain. Calculation parameters of the system are the same as in Fig. 2,  $N = 4$ , and  $\varphi = 0.1$ . The lower row [(d)–(f)] represents zoomed-in images at the short times of output wave functions in the upper row [(a)–(c)].

which these contributions are manifested, is schematically summarized in Fig. 2(a). We will now discuss it in more detail.

Single- and double- excited subradiant states manifest themselves as the long-living tails in the wave function along the edges of the calculation domain in Fig. 2(a) and along its main diagonal, respectively. The black solid and dark red curves show the two corresponding cuts in Fig. 2(b). To distinguish between single- and double-excited subradiant states, we performed calculations along the same cuts that neglect all single-excited subradiant states and include just a superradiant single-excited mode [the dotted curves in Fig. 2(b)]. Such an approximation well describes the initial fast decay of the wave functions for both curves and the tails along the main diagonal ( $t_1 = t_2$ , red dotted curve). Thus, the tails along the main diagonal can be attributed to the double-excited subradiant states. On the other hand, this approximation significantly underestimates the values of the tails of the wave function for fixed  $t_2 = 0.2/\gamma_{1D}$ , as can be seen by the comparison of the solid black and dotted gray curves in Fig. 2(b). This indicates that the tails in the solid black curve are due to the single-excited subradiant states.

The single-particle superradiant state manifests itself on the antidiagonal direction in the  $(t_1, t_2)$  plane. It should be then measured as a function of the time difference between two photons. This can be seen by comparing the solid green curve in Fig. 2(d), calculated accounting for all single-particle states, with the dashed orange one that includes only superradiant single-particle states. Such a single superradiant mode approximation correctly describes the shape of the central

peak in the full calculation. We also checked that to correctly describe the amplitude of this sharp central feature it is necessary to include all the double-excited states.

We also calculated the photon pair wave function for the case when the two incoming photons are separated by the delay time  $\tau$ . The results are shown in Fig. 3. The upper and bottom rows present the wave function calculated in the large and smaller (zoomed-in) time domains, respectively. Three columns correspond to the three values of  $\tau$ . The results in Figs. 3(a) and 3(d), when  $\tau = 0.5/\gamma_{1D}$ , look qualitatively similar to those in Fig. 4. The only difference is the absence of the signal before the last photon has arrived, that is, when  $t_1 < \tau$  or  $t_2 < \tau$ . The increase of the value of  $\tau$  leads to the modification of the transmitted photon pair wave function. The most notable modification is the suppression of the central feature at  $t_1 = t_2$ , corresponding to the two-photon bound state. Indeed, the interaction between the two photons is quenched when they do not arrive simultaneously.

### B. Duration of the transmitted pulse and the average time between two photons

As the measure of the efficiency of the dark states' excitation, we introduce the quantity

$$T = \frac{\iint dt_1 dt_2 |\psi_{t_1, t_2}^{\text{out}}|^2 t_1}{\iint dt_1 dt_2 |\psi_{t_1, t_2}^{\text{out}}|^2} \quad (11)$$

in the same way as was done in Ref. [36]. Taking into account the bosonic statistics of photons, we leave only the time of

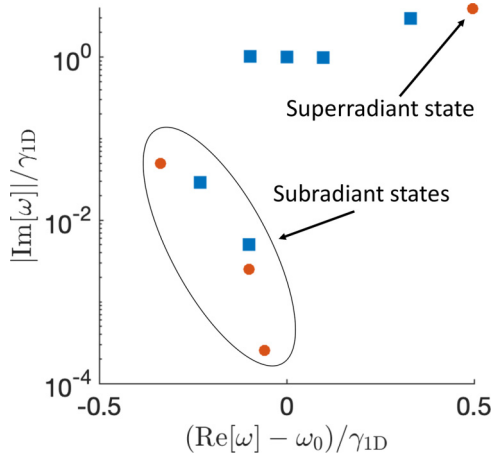


FIG. 4. Complex frequency spectrum for the following system parameters: number of qubits  $N = 4$ ; normalized period of the array  $\varphi = 0.1$ . Orange dots denote single-photon states, blue squares correspond to the two-photon states.

the one photon  $t_1$  under the integral (in general, we should look at the average times of both particles). The quantity  $T$  defined in such a way has the meaning of the duration of the transmitted pulse. Therefore, we expect that the excitation of the dark states increases the value of  $T$ . Figure 5(a) represents the dependence of the inverse duration of the transmitted pulse  $1/T$  on the number of qubits  $N$  and the period of the system  $\varphi$ . If all the qubits are placed at one point ( $\varphi = 0$ ) then a short propagating pulse excites a superradiant state. This case corresponds to the maximum values of  $1/T$  for each  $N$  in Fig. 5(a). If the qubits are periodically spaced with a normalized distance  $\varphi$  equal to  $\pi/2$ , the dark states can be excited more efficiently. Indeed, as expected, the value  $\varphi = \pi/2$  corresponds to the largest values of  $T$  (minimum values of  $1/T$ ) for each  $N$  in Fig. 5(a).

The time  $T$  becomes shorter for the larger number of qubits for a fixed period  $\varphi$  as the decay rate of the superradiant mode is equal to  $N\gamma_{1D}$ . This is also related to the Markovian approximation we use. This approximation implies the infinite speed of light, so that the increase of  $N$  and the physical length of the system does not lead to an increase of  $T$  [36].

Similarly to the average duration of the transmitted pulse, we introduce the average difference of arrival times between two transmitted photons

$$\Delta T = \frac{\iint dt_1 dt_2 |\psi_{t_1, t_2}^{\text{out}}|^2 |t_1 - t_2|}{\iint dt_1 dt_2 |\psi_{t_1, t_2}^{\text{out}}|^2}. \quad (12)$$

The general dependence of the  $\Delta T$  on the phase  $\varphi$  for the fixed numbers of qubits  $N$  looks mostly similar to the one discussed above for the duration of the transmitted pulse  $T$  [compare Figs. 5(a) and 5(b)]. In particular, when the qubits are periodically spaced with the quarter wavelength distance (corresponding to  $\varphi = \pi/2$ ), the time difference  $\Delta T$  is mainly defined by subradiant modes. In contrast, when all the qubits are located at one point ( $\varphi = 0$ ) we observe the excitation of the superradiant mode. More careful comparison between Figs. 5(b) and 5(a) reveals a qualitative difference between the dependencies of  $1/\Delta T$  and of  $1/T$  on  $N$ . While  $1/T$

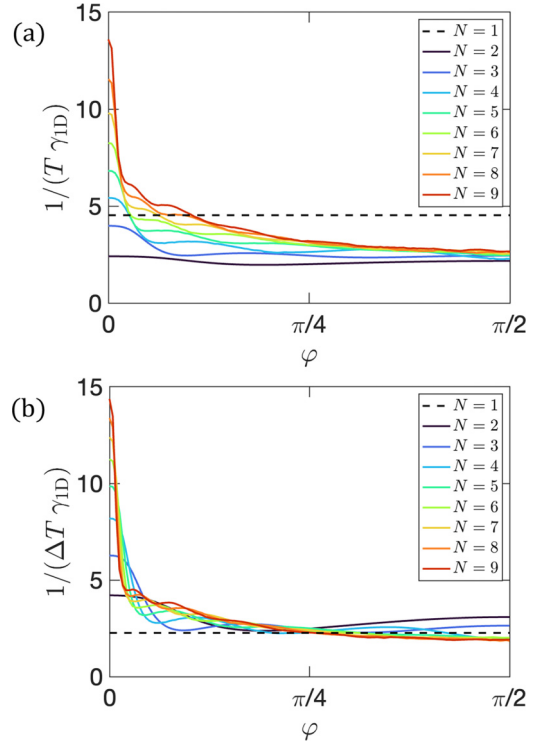


FIG. 5. Dependence of the inverse duration of the (a) transmitted pulse  $1/T$  and (b) the inverse average time between two photons  $1/\Delta T$  on the period of the system  $\varphi$  for fixed numbers of qubits  $N$ .

monotonously increases with  $N$  for all  $\varphi$ ,  $1/\Delta T$  increases with  $N$  for  $\varphi = 0$  and decreases with  $N$  for  $\varphi = \pi/2$ . As such, the  $\Delta T$  parameter looks more suitable to distinguish between the regimes, controlled by the superradiant mode ( $\varphi = 0$ ) and by the subradiant modes ( $\varphi = \pi/2$ ).

#### IV. SUMMARY

To summarize, we developed a general analytical theory for the scattering of two-photon pulses from an array of two-level atoms, coupled to the waveguide. The wave function of the scattered pulse was obtained by a convolution of the known two-photon scattering matrix in the frequency domain with the Fourier transform of the incident pulse. In the case of a pulse duration being much shorter than the spontaneous emission lifetime, we were able to obtain a general analytical result for the scattered signal. This analytical expression, while being relatively cumbersome, considerably simplifies an interpretation of the scattered signal. Namely, it becomes possible to understand the role of the qualitatively different contributions corresponding to various single-excited and double-excited eigenstates of the arrays with different radiative lifetimes (subradiant and superradiant states).

We also studied the dependence of the average time it takes the array to emit two photons when being excited resonantly on the array length and period. The emission time becomes generally shorter for longer structures, which can be explained by the formation of superradiant single-excited photon states. The longest emission times correspond to the structures with the anti-Bragg period, equal to the quarter of the wavelength

of light at the atom resonance frequency  $\lambda/4$ . This is due to the suppression of the superradiant states for the anti-Bragg structures.

Our results indicate that the time-dependent spectroscopy of photon transmission can be an interesting complementary tool to the frequency domain analysis. It would be also instructive to generalize the results for the more complicated time dependence and entanglement structure of the input pulse. While this problem has already been analyzed in the literature [15,19], the general effect of the excitation spectrum of the array on the quantum pulse transmission is far from being completely understood. For example, it would be interesting to examine what happens with the quantum light transmission through the Bragg structures with the period of  $\lambda/2$  [36] that can demonstrate strongly non-Markovian physics [26].

### ACKNOWLEDGMENT

A.V.P. acknowledges the support from the Foundation Basis.

### APPENDIX A: APPLICATION OF S-MATRIX METHOD FOR THE CALCULATION OF A DELTA-PULSE TRANSMISSION

Here we describe how to consider scattering of a short input two-photon pulse of the shape Eq. (10). Its Fourier transform (2) is given just by  $\psi_{\omega_1, \omega_2}^{\text{in}} = 1$ . Next, we define the frequency-integrated scattering matrix

$$\begin{aligned} \tilde{S}(\omega'_1, \omega'_2) &\equiv \iint \frac{d\omega_1 d\omega_2}{(2\pi)^2} S(\omega'_1, \omega'_2 \leftarrow \omega_1, \omega_2) \\ &= 2t_{\omega'_1, \omega'_2} + 2\gamma_{\text{ID}}^2 \sum_{i,j} s_i^-(\omega'_1) s_i^-(\omega'_2) Q_{ij} \\ &\quad \times \int \frac{d\omega_1}{2\pi} s_j^+(\omega_1) s_j^+(\omega'_1 + \omega'_2 - \omega_1), \end{aligned} \quad (\text{A1})$$

where  $Q = \Sigma^{-1}$  [see Eqs. (5) to (7)]. To further proceed with the frequency integration it is instructive to expand the coupling coefficients

$$s_j^{\pm}(\omega) = \sum_v \frac{s_j^{\pm, v}}{\omega_v - \omega} \quad (\text{A2})$$

as a sum of resonances at the single-excited state eigenfrequencies  $\omega_v$ . These are given just by the eigenvalues of the effective Hamiltonian matrix  $H_{mn}$ , defined in Eq. (7). Given Eq. (A2), the frequency integration in the last line of Eq. (A1) results in

$$\begin{aligned} &f_j^+(\omega'_1 + \omega'_2) \\ &\equiv \int \frac{d\omega_1}{2\pi} s_j^+(\omega_1) s_j^+(\omega'_1 + \omega'_2 - \omega_1) \\ &= - \sum_{\mu, \nu} \int \frac{d\omega_1}{2\pi} \frac{s_j^{+, \nu} s_j^{+, \mu}}{(\omega_1 - \omega_\nu)(\omega_1 + \omega_\mu - \omega'_1 - \omega'_2)} \\ &= i \sum_{\mu, \nu} \frac{s_j^{+, \nu} s_j^{+, \mu}}{\omega_\nu + \omega_\mu - \omega'_1 - \omega'_2}. \end{aligned} \quad (\text{A3})$$

To further proceed with the integration it is necessary to also expand the matrix  $Q$  over the resonant terms. The resonances correspond to the double-excited states, found from the effective Hamiltonian

$$\sum_{m'n'=1}^N (\mathcal{H} + \mathcal{U})_{mn, m'n'} \psi_{m'n'} = 2\varepsilon \psi_{mn}, \quad (\text{A4})$$

with  $\mathcal{H}_{mn, m'n'} = \delta_{mm'} H_{nn'} + \delta_{nn'} H_{mm'}$ , and  $\mathcal{U}_{mn, m'n'} = \delta_{mn} \delta_{mm'} \delta_{nn'} U$ , where  $m$  and  $n$  are the coordinates of first and second excitation. Here, the coefficient  $U$  describes the anharmonicity of the qubit potential. In the considered case of the two-level qubit, the limit  $U \rightarrow \infty$  should be taken. Then, Eq. (6) can be further simplified to

$$Q_{mn} = 2(i\varepsilon - \gamma_{\text{ID}}) \delta_{mn} + \sum_{\nu=1}^{N(N-1)/2} \frac{2id_m^{\nu} d_n^{\nu}}{\varepsilon_{\nu} - \varepsilon}, \quad (\text{A5})$$

where  $\varepsilon_{\nu}$  are the two-photon state energies found from Eq. (A4), and  $d_m^{\nu} = \mathcal{H}_{mm, m'n'} \psi_{m'n'}^{\nu}$  with the normalization condition for two-photon states being  $\sum_{m'n'} (\psi_{m'n'}^{\nu})^2 = 1$ .

Using the expansions Eqs. (A5) and (A3) the scattering matrix (A1) becomes

$$\tilde{S}(\omega'_1, \omega'_2) = 2t_{\omega'_1, \omega'_2} + 2\gamma_{\text{ID}}^2 \sum_i s_i^-(\omega'_1) s_i^-(\omega'_2) u_i(\omega'_1 + \omega'_2), \quad (\text{A6})$$

where

$$\begin{aligned} u_i(\varepsilon) &= -2(\varepsilon + i\gamma_{\text{ID}}) \sum_{\nu, \mu} \frac{s_i^{+, \nu} s_i^{+, \mu}}{(\omega_{\nu} + \omega_{\mu} - 2\varepsilon)} \\ &\quad - 2 \sum_{\kappa=1}^{N(N-1)/2} \frac{d_i^{\kappa}}{\varepsilon_{\kappa} - \varepsilon} \sum_{\nu, \mu} \frac{1}{\omega_{\nu} + \omega_{\mu} - 2\varepsilon} \\ &\quad \times \sum_{j=1}^N d_j^{\kappa} s_j^{+, \nu} s_j^{+, \mu}. \end{aligned} \quad (\text{A7})$$

To simplify the notation it is convenient to relabel the indices so that  $r = (\mu, \nu)$  and rewrite the same equation in a more general form

$$u_i(\varepsilon) = \sum_r \frac{i\varepsilon - \gamma_{\text{ID}}}{(\varepsilon_r - \varepsilon)} U_i^r + \sum_{rs} \frac{V_i^{rs}}{(\varepsilon_r - \varepsilon)(\varepsilon_s - \varepsilon)}, \quad (\text{A8})$$

where

$$U_i^r = i s_i^{+, \nu} s_i^{+, \mu} \quad (\text{A9})$$

and

$$V_i^{rs} = (-1) d_i^s \left( \sum_{j=1}^N d_j^s s_j^{+, \nu} s_j^{+, \mu} \right). \quad (\text{A10})$$

We are now in position to substitute Eq. (A6) into Eq. (4) and integrate over frequencies  $\omega_{1,2}$  to find the output wave function in the form

$$\begin{aligned} \psi_{t_1, t_2}^{\text{out}} &= \psi_{t_1, t_2}^{\text{out, coh}} + \psi_{t_1, t_2}^{\text{out, incoh}} \\ &= \frac{1}{2} \iint \frac{d\omega'_1 d\omega'_2}{(2\pi)^2} \tilde{S}(\omega'_1, \omega'_2) e^{-i\omega'_1 t_1} e^{-i\omega'_2 t_2}. \end{aligned} \quad (\text{A11})$$

The coherent part of the output wave function is given by the following expression:

$$\psi_{t_1, t_2}^{\text{out, coh}} = y(t_1)y(t_2), \quad (\text{A12})$$

with

$$y(t_1) = \int \frac{d\omega'_1}{2\pi} t(\omega'_1)e^{-i\omega'_1 t_1} = i\theta(t_1) \sum_{\mu} e^{-i\omega_{\mu} t_1} t_{\mu}, \quad (\text{A13})$$

$$y(t_2) = \int \frac{d\omega'_2}{2\pi} t(\omega'_2)e^{-i\omega'_2 t_2} = i\theta(t_2) \sum_{\nu} e^{-i\omega_{\nu} t_2} t_{\nu}. \quad (\text{A14})$$

The incoherent part of the output wave function is written as

$$\psi_{t_1, t_2}^{\text{out, incoh}} = \gamma_{\text{1D}}^2 \sum_{i, \mu, \nu} s_i^{-, \nu} s_i^{-, \mu} \left[ \sum_r U_i^r L_{\nu\mu r}(t_1, t_2) + \sum_{rs} V_i^{rs} M_{\nu\mu rs}(t_1, t_2) \right], \quad (\text{A15})$$

where

$$L_{\nu\mu r}(t_1, t_2) = \theta(t_1)\theta(t_2) \iint \frac{d\omega'_1 d\omega'_2}{(2\pi)^2} e^{-i\omega'_1 t_1} e^{-i\omega'_2 t_2} \frac{(i\varepsilon - \gamma_{\text{1D}})}{(\varepsilon_r - \varepsilon)} \frac{1}{(\omega_{\nu} - \omega'_1)(\omega_{\mu} - \omega'_2)}, \quad (\text{A16})$$

and

$$M_{\nu\mu rs}(t_1, t_2) = \theta(t_1)\theta(t_2) \iint \frac{d\omega'_1 d\omega'_2}{(2\pi)^2} e^{-i\omega'_1 t_1} e^{-i\omega'_2 t_2} \frac{1}{(\varepsilon_r - \varepsilon)(\varepsilon_s - \varepsilon)} \frac{1}{(\omega_{\nu} - \omega'_1)(\omega_{\mu} - \omega'_2)}. \quad (\text{A17})$$

For Eqs. (A13) and (A14) we use the expansion of transmission coefficient over one-particle resonant terms

$$t(\omega) = \sum_{\mu} \frac{t_{\mu}}{\omega - \omega_{\mu}}. \quad (\text{A18})$$

The integrals in Eqs. (A16) and (A17) are readily found by the Cauchy theorem, e.g., in MATHEMATICA. As a result, we obtain the following expressions:

$$L_{\nu\mu r}(t_1, t_2) = \theta(t_1)\theta(t_2) [(i\varepsilon_r - \gamma_{\text{1D}})(\theta(t_1 - t_2)e^{-i\omega_{\nu}(t_1 - t_2) - 2i\varepsilon_r t_2} + \theta(t_2 - t_1)e^{-i\omega_{\mu}(t_2 - t_1) - 2i\varepsilon_r t_1}) - [i(\omega_{\mu} + \omega_{\nu})/2 - \gamma_{\text{1D}}]e^{-i\omega_{\nu} t_1 - i\omega_{\mu} t_2}] \frac{1}{\varepsilon_r - (\omega_{\nu} + \omega_{\mu})/2}, \quad (\text{A19})$$

$$M_{\nu\mu rs}(t_1, t_2) = \theta(t_1)\theta(t_2)\theta(t_2 - t_1) \{ [\varepsilon_r - (\omega_{\mu} + \omega_{\nu})/2]e^{-i\omega_{\mu}(t_2 - t_1) - 2i\varepsilon_s t_1} - [\varepsilon_s - (\omega_{\mu} + \omega_{\nu})/2]e^{-i\omega_{\mu}(t_2 - t_1) - 2i\varepsilon_s t_1} - (\varepsilon_r - \varepsilon_s)e^{-i\omega_{\nu} t_1 - i\omega_{\mu} t_2} \} \frac{1}{[\varepsilon_r - (\omega_{\nu} + \omega_{\mu})/2][\varepsilon_s - (\omega_{\nu} + \omega_{\mu})/2](\varepsilon_r - \varepsilon_s)} + (t_1 \leftrightarrow t_2, \omega_{\nu} \leftrightarrow \omega_{\mu}). \quad (\text{A20})$$

## APPENDIX B: TWO SHORT ONE-PHOTON PULSES WITH A TIME DELAY

In this Appendix, we discuss how to describe the scattering of two short one-photon pulses with a time delay. Such a pulse can be approximated by a product of two  $\delta$  functions with the time delay  $\tau$ :

$$\psi_{t_1, t_2}^{\text{in}} = \delta(t_1 - \tau)\delta(t_2) + \delta(t_1)\delta(t_2 - \tau), \quad (\text{B1})$$

which is symmetrized in the time domain as two photons are indistinguishable due to their bosonic nature.

For simplicity, we first consider the initial pulse in the form

$$\psi_{t_1, t_2}^{\text{in}} = \delta(t_1 - \tau)\delta(t_2). \quad (\text{B2})$$

Its Fourier transform is then given by  $e^{i\omega_1 \tau}$ . We repeat the steps outlined in Appendix A but with an incident pulse of a shape given by Eq. (B2).

The output wave function assumes the form

$$\psi_{t_1, t_2}^{\text{out}} = \psi_{t_1, t_2}^{\text{out, coh}} + \psi_{t_1, t_2}^{\text{out, incoh}}, \quad (\text{B3})$$

with the coherent part is given by

$$\psi_{t_1, t_2}^{\text{out, coh}} = y(t_1)y(t_2), \quad (\text{B4})$$

where

$$y(t_1) = \int \frac{d\omega'_1}{2\pi} t(\omega'_1) e^{i\omega'_1 \tau} e^{-i\omega'_1 t_1} = i\theta(t_1 - \tau) \sum_{\mu} e^{-i\omega'_1(t_1 - \tau)} t_{\mu}, \quad (\text{B5})$$

$$y(t_2) = \int \frac{d\omega'_2}{2\pi} t(\omega'_2) e^{-i\omega'_2 t_2} = i\theta(t_2) \sum_{\nu} e^{-i\omega'_2 t_2} t_{\nu}. \quad (\text{B6})$$

The incoherent part reads as

$$\psi_{t_1, t_2}^{\text{out, incoh}} = \gamma_{\text{ID}}^2 \sum_{i, \mu, \nu} s_i^{-, \nu} s_i^{-, \mu} \left[ \sum_r U_i^r L_{\nu\mu r}(t_1, t_2) + \sum_{rs} V_i^{rs} M_{\nu\mu rs}(t_1, t_2) \right], \quad (\text{B7})$$

where

$$U_i^r = i s_i^{+, \nu} s_i^{+, \mu} e^{-i\omega_{\nu} \tau}, \quad (\text{B8})$$

$$V_i^{rs} = (-1) d_i^s \left( \sum_{j=1}^N d_j^s s_j^{+, \nu} s_j^{+, \mu} \right) e^{-i\omega_{\nu} \tau}, \quad (\text{B9})$$

$$\begin{aligned} L_{\nu\mu r}(t_1, t_2) &= \iint \frac{d\omega'_1 d\omega'_2}{(2\pi)^2} e^{-i\omega'_1 t_1} e^{-i\omega'_2 t_2} e^{i2\varepsilon\tau} \frac{(i\varepsilon - 1)}{(\varepsilon_r - \varepsilon)} \frac{1}{(\omega_{\nu} - \omega'_1)(\omega_{\mu} - \omega'_2)} \\ &= \iint \frac{d\omega'_1 d\omega'_2}{(2\pi)^2} e^{-i\omega'_1(t_1 - \tau)} e^{-i\omega'_2(t_2 - \tau)} \frac{(i\varepsilon - 1)}{(\varepsilon_r - \varepsilon)} \frac{1}{(\omega_{\nu} - \omega'_1)(\omega_{\mu} - \omega'_2)}, \end{aligned} \quad (\text{B10})$$

and

$$\begin{aligned} M_{\nu\mu rs}(t_1, t_2) &= \iint \frac{d\omega'_1 d\omega'_2}{(2\pi)^2} e^{-i\omega'_1 t_1} e^{-i\omega'_2 t_2} e^{i2\varepsilon\tau} \frac{1}{(\varepsilon_r - \varepsilon)(\varepsilon_s - \varepsilon)} \frac{1}{(\omega_{\nu} - \omega'_1)(\omega_{\mu} - \omega'_2)} \\ &= \iint \frac{d\omega'_1 d\omega'_2}{(2\pi)^2} e^{-i\omega'_1(t_1 - \tau)} e^{-i\omega'_2(t_2 - \tau)} \frac{1}{(\varepsilon_r - \varepsilon)(\varepsilon_s - \varepsilon)} \frac{1}{(\omega_{\nu} - \omega'_1)(\omega_{\mu} - \omega'_2)}. \end{aligned} \quad (\text{B11})$$

Evaluating the integrals in Eqs. (B10) and (B11) we obtain the expressions which are the same as Eqs. (A19) and (A20) up to the following substitution  $t_1 \rightarrow t_1 - \tau$ ,  $t_2 \rightarrow t_2 - \tau$  in the right parts of the equations.

The second term in Eq. (B1) provides the same output wave function up to the exchange of times  $t_1 \leftrightarrow t_2$ . The resulting output wave function for the input pulse in the form of Eq. (B1) is given by the sum of two output terms.

- 
- [1] A. S. Sheremet, M. I. Petrov, I. V. Iorsh, A. V. Poshakinskiy, and A. N. Poddubny, Waveguide quantum electrodynamics: Collective radiance and photon-photon correlations, *Rev. Mod. Phys.* **95**, 015002 (2023).
- [2] D. Roy, C. M. Wilson, and O. Firstenberg, Colloquium: Strongly interacting photons in one-dimensional continuum, *Rev. Mod. Phys.* **89**, 021001 (2017).
- [3] A. S. Prasad, J. Hinney, S. Mahmoodian, K. Hammerer, S. Rind, P. Schneeweiss, A. S. Sørensen, J. Volz, and A. Rauschenbeutel, Correlating photons using the collective nonlinear response of atoms weakly coupled to an optical mode, *Nat. Photonics* **14**, 719 (2020).
- [4] J. Hinney, A. S. Prasad, S. Mahmoodian, K. Hammerer, A. Rauschenbeutel, P. Schneeweiss, J. Volz, and M. Schemmer, Unraveling Two-Photon Entanglement via the Squeezing Spectrum of Light Traveling through Nanofiber-Coupled Atoms, *Phys. Rev. Lett.* **127**, 123602 (2021).
- [5] C. Liedl, S. Pucher, F. Tebbenjohanns, P. Schneeweiss, and A. Rauschenbeutel, Collective Radiation of a Cascaded Quantum System: From Timed Dicke States to Inverted Ensembles, *Phys. Rev. Lett.* **130**, 163602 (2023).
- [6] C. Liedl, F. Tebbenjohanns, C. Bach, S. Pucher, A. Rauschenbeutel, and P. Schneeweiss, Observation of superradiant bursts in waveguide QED, [arXiv:2211.08940](https://arxiv.org/abs/2211.08940).
- [7] B. Kannan, A. Almanakly, Y. Sung, A. D. Paolo, D. A. Rower, J. Braumüller, A. Melville, B. M. Niedzielski, A. Karamlou, K. Serniak, A. Vepsäläinen, M. E. Schwartz, J. L. Yoder, R. Winik, J. I.-J. Wang, T. P. Orlando, S. Gustavsson, J. A. Grover, and W. D. Oliver, On-demand directional microwave photon emission using waveguide quantum electrodynamics, *Nat. Phys.* **19**, 394 (2023).
- [8] V. I. Yudson and V. I. Rupasov, Exact Dicke superradiance theory: Bethe wave functions in the discrete atom model, *Zh. Eksp. Teor. Fiz.* **86**, 819 (1984) [*Sov. Phys. JETP* **59**, 478 (1984)].
- [9] V. I. Yudson and P. Reineker, Multiphoton scattering in a one-dimensional waveguide with resonant atoms, *Phys. Rev. A* **78**, 052713 (2008).
- [10] J.-T. Shen and S. Fan, Strongly Correlated Two-Photon Transport in a One-Dimensional Waveguide Coupled

- to a Two-Level System, *Phys. Rev. Lett.* **98**, 153003 (2007).
- [11] D. Roy, Cascaded two-photon nonlinearity in a one-dimensional waveguide with multiple two-level emitters, *Sci. Rep.* **3**, 2337 (2013).
- [12] S. Mahmoodian, M. Čepulkovskis, S. Das, P. Lodahl, K. Hammerer, and A. S. Sørensen, Strongly Correlated Photon Transport in Waveguide Quantum Electrodynamics with Weakly Coupled Emitters, *Phys. Rev. Lett.* **121**, 143601 (2018).
- [13] S. Mahmoodian, G. Calajó, D. E. Chang, K. Hammerer, and A. S. Sørensen, Dynamics of Many-Body Photon Bound States in Chiral Waveguide QED, *Phys. Rev. X* **10**, 031011 (2020).
- [14] Z. Chen, Y. Zhou, and J.-T. Shen, Correlation signatures for a coherent three-photon scattering in waveguide quantum electrodynamics, *Opt. Lett.* **45**, 2559 (2020).
- [15] G. Calajó and D. E. Chang, Emergence of solitons from many-body photon bound states in quantum nonlinear media, *Phys. Rev. Res.* **4**, 023026 (2022).
- [16] O. A. Iversen and T. Pohl, Self-ordering of individual photons in waveguide QED and Rydberg-atom arrays, *Phys. Rev. Res.* **4**, 023002 (2022).
- [17] E. V. Stolyarov, Few-photon Fock-state wave packet interacting with a cavity-atom system in a waveguide: Exact quantum state dynamics, *Phys. Rev. A* **99**, 023857 (2019).
- [18] A. H. Kiilerich and K. Mølmer, Quantum interactions with pulses of radiation, *Phys. Rev. A* **102**, 023717 (2020).
- [19] F. Yang, M. M. Lund, T. Pohl, P. Lodahl, and K. Mølmer, Deterministic Photon Sorting in Waveguide QED Systems, *Phys. Rev. Lett.* **128**, 213603 (2022).
- [20] B. Olmos, G. Buonaiuto, P. Schneeweiss, and I. Lesanovsky, Interaction signatures and non-gaussian photon states from a strongly driven atomic ensemble coupled to a nanophotonic waveguide, *Phys. Rev. A* **102**, 043711 (2020).
- [21] S. Cardenas-Lopez, S. J. Masson, Z. Zager, and A. Asenjo-Garcia, Many-Body Superradiance and Dynamical Mirror Symmetry Breaking in Waveguide QED, *Phys. Rev. Lett.* **131**, 033605 (2023).
- [22] Y.-X. Zhang and K. Mølmer, Theory of Subradiant States of a One-Dimensional Two-Level Atom Chain, *Phys. Rev. Lett.* **122**, 203605 (2019).
- [23] Y. Ke, A. V. Poshakinskiy, C. Lee, Y. S. Kivshar, and A. N. Poddubny, Inelastic Scattering of Photon Pairs in Qubit Arrays with Subradiant States, *Phys. Rev. Lett.* **123**, 253601 (2019).
- [24] A. V. Poshakinskiy, J. Zhong, Y. Ke, N. A. Olekhno, C. Lee, Y. S. Kivshar, and A. N. Poddubny, Quantum hall phases emerging from atom-photon interactions, *npj Quantum Inf.* **7**, 34 (2021).
- [25] A. V. Poshakinskiy and A. N. Poddubny, Dimerization of Many-Body Subradiant States in Waveguide Quantum Electrodynamics, *Phys. Rev. Lett.* **127**, 173601 (2021).
- [26] A. V. Poshakinskiy and A. N. Poddubny, Quantum Bornmann effect for dissipation-immune photon-photon correlations, *Phys. Rev. A* **103**, 043718 (2021).
- [27] D. Kornovan, A. Poddubny, and A. Poshakinskiy, Long persistent anticorrelations in few-qubit arrays, [arXiv:2303.02085](https://arxiv.org/abs/2303.02085) [Phys. Rev. A (to be published)].
- [28] J. D. Brehm, A. N. Poddubny, A. Stehli, T. Wolz, H. Rotzinger, and A. V. Ustinov, Waveguide band-gap engineering with an array of superconducting qubits, *npj Quantum Mater.* **6**, 10 (2021).
- [29] M. Zanner, T. Orell, C. M. F. Schneider, R. Albert, S. Oleschko, M. L. Juan, M. Silveri, and G. Kirchmair, Coherent control of a multi-qubit dark state in waveguide quantum electrodynamics, *Nat. Phys.* **18**, 538 (2022).
- [30] J. D. Brehm, R. Gebauer, A. Stehli, A. N. Poddubny, O. Sander, H. Rotzinger, and A. V. Ustinov, Slowing down light in a qubit metamaterial, *Appl. Phys. Lett.* **121**, 204001 (2022).
- [31] H. L. Jeannic, A. Tiranov, J. Carolan, T. Ramos, Y. Wang, M. H. Appel, S. Scholz, A. D. Wieck, A. Ludwig, N. Rotenberg, L. Midolo, J. J. García-Ripoll, A. S. Sørensen, and P. Lodahl, Dynamical photon-photon interaction mediated by a quantum emitter, *Nat. Phys.* **18**, 1191 (2022).
- [32] T. Caneva, M. T. Manzoni, T. Shi, J. S. Douglas, J. I. Cirac, and D. E. Chang, Quantum dynamics of propagating photons with strong interactions: A generalized input-output formalism, *New J. Phys.* **17**, 113001 (2015).
- [33] M. Laakso and M. Pletyukhov, Scattering of Two Photons from Two Distant Qubits: Exact Solution, *Phys. Rev. Lett.* **113**, 183601 (2014).
- [34] Y.-L. L. Fang, H. Zheng, and H. U. Baranger, One-dimensional waveguide coupled to multiple qubits: Photon-photon correlations, *EPJ Quantum Technol.* **1**, 3 (2014).
- [35] A. V. Poshakinskiy and A. N. Poddubny, Biexciton-mediated superradiant photon blockade, *Phys. Rev. A* **93**, 033856 (2016).
- [36] A. V. Poshakinskiy, A. N. Poddubny, and S. A. Tarasenko, Reflection of short polarized optical pulses from periodic and aperiodic multiple quantum well structures, *Phys. Rev. B* **86**, 205304 (2012).